High-Order Mode Application of Spoof Surface Plasmon Polaritons in Bandpass Filter Design

Yiqun Liu, Kai-Da Xu, *Senior Member, IEEE*, Ying-Jiang Guo, and Qiang Chen, *Senior Member, IEEE*

***Abstract*— In this letter, high-order mode dispersion of a novel spoof surface plasmon polariton (SSPP) unit cell is reported, which has excellent bandpass propagation feature. Its asymptotic frequency and intersection frequency with light line can be independently manipulated by changing the geometric parameters of the slot in proposed SSPP unit cell. In order to validate the feasibility of high-order mode of SSPPs applied in the design of bandpass filters, two SSPP waveguides based on the method with different bandwidths are fabricated and measured. No mode-conversion transition part is introduced in the procedure of waveguide design which avoids extra addition of layout area and reduces complexity of devices. The measurements show that the proposed SSPP waveguide based on high-order mode characteristics can achieve bandpass signal propagation smoothly with controllable bandwidth.**

***Index Terms*— High order mode, bandpass filter, spoof surface plasmon polaritons, waveguide.**

I. Introduction

SURFACE plasmon polaritons (SPPs) are surface electromagnetic (EM) waves which can be excited and effectively propagated along metal-dielectric surface with decayed exponentially in the vertical direction to the surface [1]. Unfortunately, SPPs are tendentiously replaced by Sommerfeld or Zenneck surface waves which have weak surface confinement property in terahertz and microwave frequencies [2]–[4] for the reason of metal behavior resembling PEC. In recent years, the appearance of spoof SPPs (SSPPs) bridges the field of SPPs and terahertz or even lower frequency [5]–[7]. In particular, the planar SSPPs which have similar ability of field confinement and adjustable dispersion characteristics are widely used in the design of antennas [8], [9], filters [10]–[12], power dividers [13], and frequency splitters [14], [15].

Manuscript received December 4, 2020; revised February 9, 2021; accepted February 28, 2021. Date of publication March 4, 2021; date of current version March 10, 2021. This work was supported in part by the FY2019 JSPS Postdoctoral Fellowship for Research in Japan under Grant P19350 and in part by the Grant-in-Aid for JSPS Research Fellow under Grant JP19F19350. *(Corresponding author: Kai-Da Xu.)*

Yiqun Liu is with the School of Information and Communications Engineering, Xi'an Jiaotong University, Xi'an 710049, China.

Kai-Da Xu is with the School of Information and Communications Engineering, Xi'an Jiaotong University, Xi'an 710049, China, and also with the Department of Communications Engineering, Graduate School of Engineering, Tohoku University, Sendai 980-8579, Japan (e-mail: kaidaxu@ieee.org).

Ying-Jiang Guo is with the Microsystem and Terahertz Research Center, China Academy of Engineering Physics, Chengdu 610200, China.

Qiang Chen is with the Department of Communications Engineering, Graduate School of Engineering, Tohoku University, Sendai 980-8579, Japan.

Color versions of one or more figures in this letter are available at https://doi.org/10.1109/LPT.2021.3063522.

Digital Object Identifier 10.1109/LPT.2021.3063522

However, most of aforementioned works focus on the fundamental mode based SSPPs design that requires extra mode-conversion transition, and few investigations have been made on the application of high-order mode SSPPs so far [16]. On the other hand, even though some works on high-order mode SSPPs have been researched such as the one in [17], only SSPP waveguide is designed without any other device applications. Therefore, it is highly worthy to investigate the applications of the high-order mode SSPPs.

In this letter, a new SSPP structure is presented through embedding slots into the conventional grating metallic strip SSPP waveguide. The high-order mode characteristics of the proposed SSPPs are further investigated. The relations between geometric parameters of slots and dispersion characteristics are analyzed. It is found that the proposed SSPP structure can be easily applied in the design of bandpass filter (BPF) and effectively increase the adjustability of bandwidth compared with the conventional one.

II. High-Order Mode Characteristics of SSPPs

In this section, a novel SSPP unit cell is structured as shown in Fig. 1(a) by embedding a narrow slot in the middle stub of the conventional SSPP unit cell. Two different groups of SSPP unit cells are investigated to study the high-order mode characteristics of the new SSPP unit cell, where each group contains the SSPP unit cells with narrow slot and without slot (i.e., the conventional one) for characteristic comparisons. Both groups of SSPP unit cells are designed on the FSD220G substrate ($\varepsilon_r = 2.2$, tan$\delta = 0.0009$, thickness of 0.127 mm) with metallic ground plane on the back of substrate to improve electromagnetic field confinement ability of SSPPs. Due to the copper is generally regarded as PEC at microwave frequency, SSPP conductor is set as a PEC material with 18 um conductor thickness. All geometrical parameters are given in Table I, where the period is p, the width of stub is w, the length of stub is h, the length and width of slot are h_1 and w_1, respectively.

The fundamental mode (Mode 0) and the first high-order mode (Mode 1) of SSPP unit cells for both groups are depicted in Fig. 1(b). Same as those of the conventional SSPP unit cell, the asymptotic frequencies of the proposed SSPP unit cell for both modes are also affected by the stub length h. The higher value of h is set, the lower asymptotic frequencies of dispersion curves will be obtained. Considering high-order mode excitation [18], [19] and wide tunability of the inserted slot length, the stub length h is chosen as 13 and 15 mm for the two cases. As shown in Fig. 1(b), the asymptotic frequencies

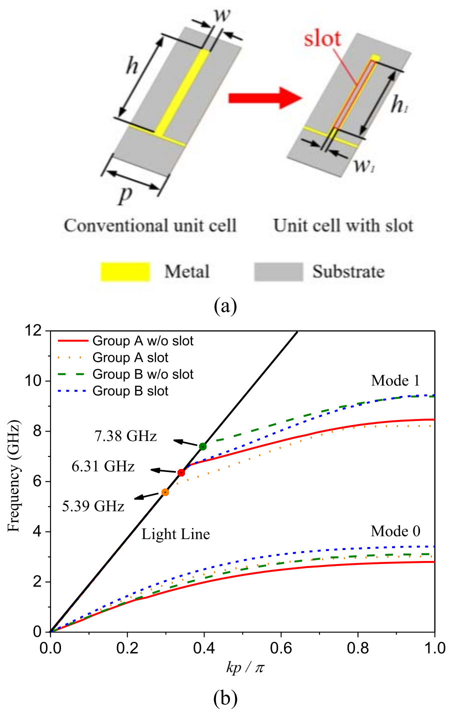

Fig. 1. (a) Layouts of two types of SSPP unit cells. The front and back metal parts are attached on both sides of the substrate. (b) Dispersion characteristics of two groups of SSPP unit cells using TM mode. Each group contains conventional one and SSPP unit cell with slot.

TABLE I
SSPP UNIT CELL PARAMETERS (UNIT: mm)

Parameter	p	w	h	h_1	w_1
Group A (slotted)	7.8	1.2	15	13	0.9
Group A (w/o slot)	7.8	1.2	15	-	-
Group B (slotted)	7.8	1.2	13	11	0.9
Group B (w/o slot)	7.8	1.2	13	-	-

of the dispersion curves of the Group B with $h = 13$ mm are higher than those of the Group A with $h = 15$ mm, which are more obvious for high-order modes of the two types of SSPP unit cells. For two groups, the frequencies of the intersection points between the Mode 1 dispersion curves and light line in free space are obviously decreased from 6.31 GHz and 7.38 GHz to 5.39 GHz and 6.31 GHz, respectively, after inserting the narrow slot. The insertion of narrow slot improves the operating bandwidth significantly if the Mode 1 is applied in the design of BPF. Moreover, it is a key point that the Mode 0 and Mode 1 have no overlapping part, indicating the single mode propagation is available and it is feasible to use the high-order mode for the design of BPF.

In order to verify the above assumption, a simple SSPP waveguide without transition part is constructed as shown in Fig. 3(a). The SSPP unit cell with 15 mm of stub length is chosen as the design prototype, i.e., Group A, and only parameter h_1 can be adjustable in the procedure of comparisons. The first part of the waveguide is a microstrip line with

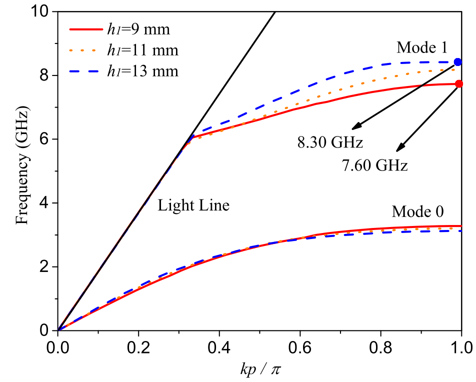

Fig. 2. Dispersion curves of the proposed SSPP unit cell (slotted one in Group A) against different slot lengths.

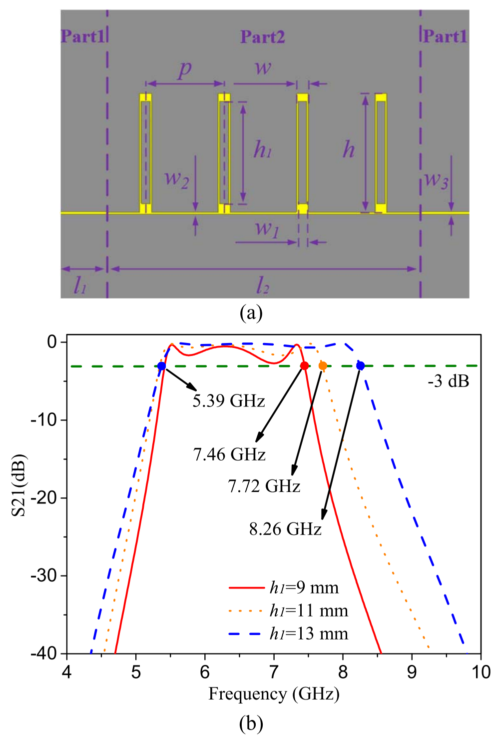

Fig. 3. (a) Waveguide configuration and (b) simulated S-parameters of the high-order SSPP waveguide with parameter h_1 variations from 9 mm to 13 mm.

TABLE II
SSPP UNIT CELL PARAMETERS (UNIT: mm)

Parameter	p	w	h	w_1	w_2	w_3	l_1	l_2
Value	7.8	1.2	15	0.9	0.3	0.38	9.4	31.2

$w_3 = 0.38$ mm for 50 Ω characteristic impedance matching and the second part is the SSPP structure containing four identical unit cells. The back of substrate is covered by the metallic ground plane to strengthen field confinement of SSPP waveguide. All other parameters of waveguide are fixed, as tabulated in Table II. Although there is no transition structure for the conversion from quasi-TEM mode to SSPP mode, good performance of passband generated by the first high-order mode still can be achieved.

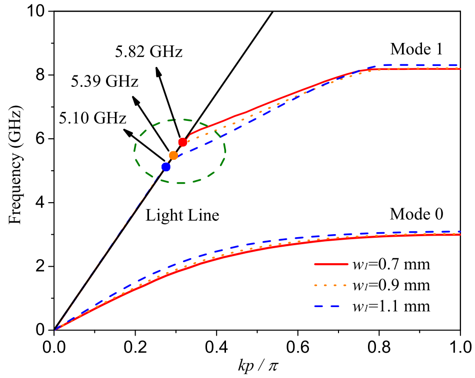

Fig. 4. Dispersion curves of the proposed SSPP unit cell (Group A) against different slot widths.

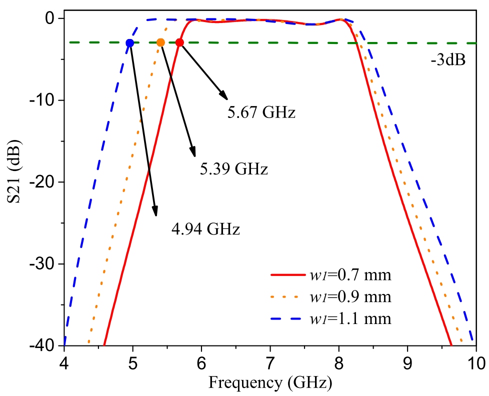

Fig. 5. Simulated S-parameters of the high-order SSPP waveguide with parameter w_1 variations from 0.7 mm to 1.1 mm, where $h_1 = 13$ mm and other parameters are shown in Table II.

As shown in Fig. 3(b), with the increase of slot length, the upper cut-off frequency corresponding to -3 dB of the passband changes from 7.46 GHz to 8.26 GHz, while the lower cut-off frequency has no obvious change. These two frequency points are basically consistent with the asymptotic frequencies of Mode 1 in Fig. 2, proportional to the slot lengths. Moreover, about 38% of bandwidth adjustment for this case can be achieved by changing the slot length from 9 mm to 13 mm.

Then, the relations between dispersion characteristics of the proposed SSPP unit cell and slot width are studied. As shown in Fig. 4, the intersection point of the Mode 1 dispersion curve with light line decreases from 5.82 GHz to 5.10 GHz when the slot width increases from 0.7 mm to 1.1 mm, while the asymptotic frequency of the dispersion curve remains almost unchanged. Therefore, the lower cut-off frequency of BPF using the proposed SSPPs can be adjusted by varying slot width, which is validated by the simulations in Fig. 5.

From the above analysis, we can draw the conclusion that the lower and upper cut-off frequencies of the passband can be independently adjusted by the slot width and length, respectively, in the design of BPF using the proposed high-order SSPP waveguide. In order to further study the high-order mode propagation characteristics of the SSPP waveguide, Fig. 6 illustrates simulated electric field distributions at 3.5 GHz (out-of-band) and 7.0 GHz (in band). It can be seen that the energy is effectively transmitted from the input port to output port at 7 GHz, while it suffers from propagation attenuation quickly at 3.5 GHz.

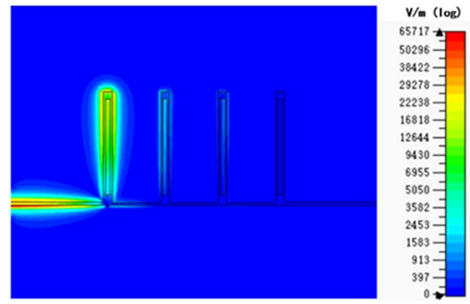

(a)

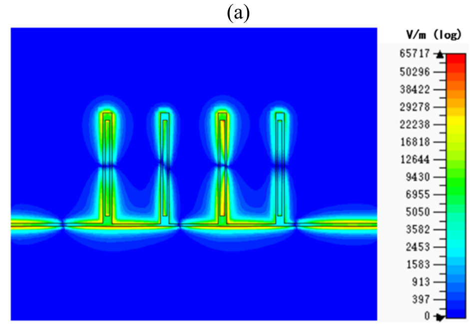

(b)

Fig. 6. Simulated electric field distributions of the SSPP waveguide at (a) 3.5 GHz and (b) 7.0 GHz.

TABLE III
SSPP UNIT CELL PARAMETERS (UNIT: mm)

Parameter	p	w	h	h_1	w_1	w_2	w_3	l_1	l_2
WG I	7.3	1.1	13	10	0.3	0.33	0.38	6	23
WG II	7.3	0.6	15	13	0.3	0.33	0.38	9	22.5

III. IMPLEMENTATION RESULTS

Based on the relations between high-order mode dispersion characteristics of the proposed SSPP unit cell and the geometrical variations of slot, Waveguide I and Waveguide II with different bandwidths for the applications of BPFs are designed and fabricated as shown in Fig. 7(a) and Fig. 7(b), respectively. All detailed parameters of these two waveguides are tabulated in Table III.

Fig. 7(c) and Fig. 7(d) show the comparisons between the simulated and measured S-parameters of these two waveguides, where good agreement between the simulations and measurements can be observed. The discrepancies between the simulated and measured results for insertion losses are likely due to the fabrication tolerance and ohmic losses of metal strips which are not included in the electromagnetic simulations. In Fig. 7(c), Waveguide I can achieve the bandwidth of 2.9 GHz with the upper and lower cut-off frequencies at 9.5 GHz and 6.6 GHz respectively, and the lowest insertion loss in passband is about 1.48 dB. In contrast, the bandwidth of Waveguide II is 3.38 GHz with upper and lower cut-off frequencies at 6.1 GHz and 9.48 GHz, respectively, and the lowest bandpass insertion loss is 1.46 dB.

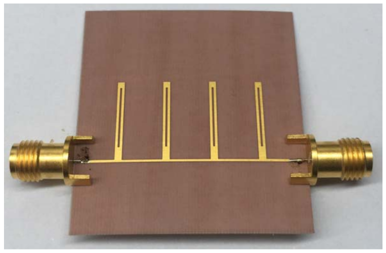

(a)

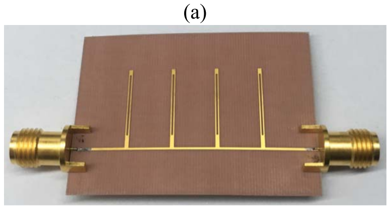

(b)

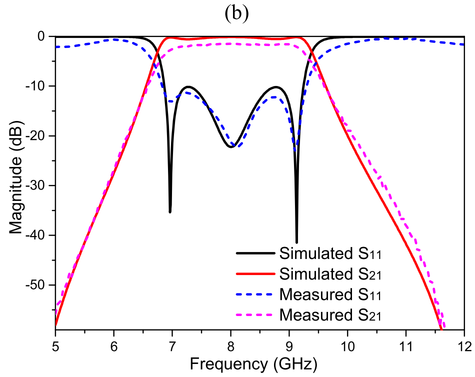

(c)

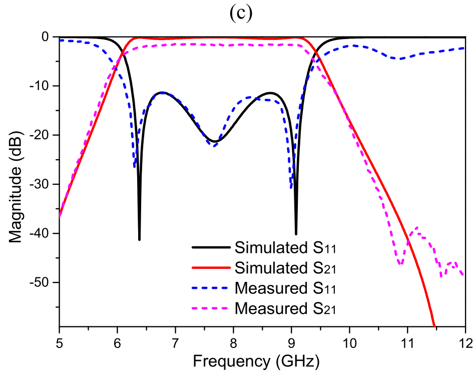

(d)

Fig. 7. Fabricated samples of (a) Waveguide I and (b) Waveguide II. Simulated and measured S-parameters of (c) Waveguide I and (d) Waveguide II.

It should be noted that the bandwidth of Waveguide II is wider than that of Waveguide I with nearly same upper cut-off frequency, which is attributed to two reasons. On the one hand, the Waveguide II has larger stub length than the Waveguide I, which causes smaller lower and upper cut-off frequencies for BPF design, as validated in Fig. 1. On the other hand, longer slots embedded into the SSPP unit cells pull up the asymptotic frequency for compensating the decrease of the upper cut-off frequency caused by the increase of the stub length.

IV. Conclusion

In this letter, the high-order dispersion characteristics of proposed SSPP unit cell have been studied, dependent on the geometrical parameters of the stub and slot of the SSPP waveguide. Compared with the conventional SSPP structure, the proposed one can easily design the BPFs with different bandwidths using high-order mode. The passband lower and upper cut-off frequencies of BPF can be independently adjusted by the slot width and length, respectively. Good agreement between the simulations and experimental results demonstrates the feasibility of the SSPP high-order mode applied in BPF design.

References

[1] W. L. Barnes, A. Dereux, and T. W. Ebbesen, “Surface plasmon subwavelength optics,” *Nature*, vol. 424, no. 6950, pp. 824–830, Aug. 2003.

[2] J. R. Wait, “The ancient and modern history of EM ground-wave propagation,” *IEEE Antennas Propag. Mag.*, vol. 40, no. 5, pp. 7–24, Oct. 1998.

[3] M. Wächter, M. Nagel, and H. Kurz, “Frequency-dependent characterization of THz Sommerfeld wave propagation on single-wires,” *Opt. Exp.*, vol. 13, no. 26, pp. 10815–10822, 2005.

[4] K.-D. Xu, H. Luyen, and N. Behdad, “A decoupling and matching network design for single- and dual-band two-element antenna arrays,” *IEEE Trans. Microw. Theory Techn.*, vol. 68, no. 9, pp. 3986–3999, Sep. 2020.

[5] J. B. Pendry, “Mimicking surface plasmons with structured surfaces,” *Science*, vol. 305, no. 5685, pp. 847–848, Aug. 2004.

[6] F. J. Garcia-Vidal, L. Martin-Moreno, and J. B. Pendry, “Surfaces with holes in them: New plasmonic metamaterials,” *J. Opt. A: Pure Appl. Opt.*, vol. 7, pp. S97–S101, 2005.

[7] K.-D. Xu *et al.*, “On-chip GaAs-based spoof surface plasmon polaritons at millimeter-wave regime,” *IEEE Photon. Technol. Lett.*, vol. 33, no. 5, pp. 255–258, Mar. 1, 2021.

[8] W. Feng, Y. Feng, W. Yang, W. Che, and Q. Xue, “High-performance filtering antenna using spoof surface plasmon polaritons,” *IEEE Trans. Plasma Sci.*, vol. 47, no. 6, pp. 2832–2837, Jun. 2019.

[9] X.-F. Zhang, J. Fan, and J.-X. Chen, “High gain and high-efficiency millimeter-wave antenna based on spoof surface plasmon polaritons,” *IEEE Trans. Antennas Propag.*, vol. 67, no. 1, pp. 687–691, Jan. 2019.

[10] Y. J. Guo, K. D. Xu, Y. H. Liu, and X. H. Tang, “Novel surface plasmon polariton waveguides with enhanced field confinement for microwave-frequency ultra-wideband bandpass filters,” *IEEE Access*, vol. 6, pp. 10249–10256, Feb. 2018.

[11] K.-D. Xu, F. Zhang, Y. Guo, L. Ye, and Y. Liu, “Spoof surface plasmon polaritons based on balanced coplanar stripline waveguides,” *IEEE Photon. Technol. Lett.*, vol. 32, no. 1, pp. 55–58, Jan. 1, 2020.

[12] Y.-J. Guo, K.-D. Xu, X. Deng, X. Cheng, and Q. Chen, “Millimeter-wave on-chip bandpass filter based on spoof surface plasmon polaritons,” *IEEE Electron Device Lett.*, vol. 41, no. 8, pp. 1165–1168, Aug. 2020.

[13] J. Wang, L. Zhao, Z. C. Hao, X. P. Shen, and T. J. Cui, “Splitting spoof surface plasmon polaritons to different directions with high efficiency in ultra-wideband frequencies,” *Opt. Lett.*, vol. 44, no. 13, pp. 3374–3377, Jul. 2019.

[14] X. Gao *et al.*, “Ultrathin dual-band surface plasmonic polariton waveguide and frequency splitter in microwave frequencies,” *Appl. Phys. Lett.*, vol. 102, no. 15, Apr. 2013, Art. no. 151912.

[15] C. Han, Z. H. Wang, Y. Y. Chu, X. D. Zhao, and X. R. Zhang, “Compact flexible multifrequency splitter based on plasmonic graded metallic grating arc waveguide,” *Opt. Lett.*, vol. 43, no. 8, pp. 1898–1901, 2018.

[16] K.-D. Xu, S. Lu, Y.-J. Guo, and Q. Chen, “High-order mode of spoof surface plasmon polaritons and its application in bandpass filters,” *IEEE Trans. Plasma Sci.*, vol. 49, no. 1, pp. 269–275, Jan. 2021.

[17] D. Zhang, K. Zhang, Q. Wu, R. Dai, and X. Sha, “Broadband high-order mode of spoof surface plasmon polaritons supported by compact complementary structure with high efficiency,” *Opt. Lett.*, vol. 43, no. 13, pp. 3176–3179, 2018.

[18] T. Jiang, L. Shen, X. Zhang, and L.-X. Ran, “High-order modes of spoof surface plasmon polaritons on periodically corrugated metal surfaces,” *Prog. Electromagn. Res. M*, vol. 8, pp. 91–102, 2009.

[19] X. Liu, Y. Feng, B. Zhu, J. Zhao, and T. Jiang, “High-order modes of spoof surface plasmonic wave transmission on thin metal film structure,” *Opt. Exp.*, vol. 21, no. 25, pp. 31155–31165, 2013.